



Using Sputter Deposition to Increase CO Tolerance in a Proton-Exchange Membrane Fuel Cell

Andrew T. Haug,^{a,*} Ralph E. White,^{a,**,z} John W. Weidner,^{a,***} Wayne Huang,^b Steven Shi,^{b,***} Narender Rana,^c Stephan Grunow,^c Timothy C. Stoner,^c and Alain E. Kaloyeros^c

^aCenter for Electrochemical Engineering, Department of Chemical Engineering, University of South Carolina, Columbia, South Carolina 29208, USA

^bPlug Power, Incorporated, Latham, New York 12110, USA

^cEnergy and Environment Applications Center, Institute for Materials, and School of Nanosciences and Engineering, State University of New York at Albany, Albany, New York 12203, USA

Placing a layer of Ru atop a Pt anode increases the carbon monoxide tolerance of proton-exchange membrane fuel cells when oxygen is added to the fuel stream. Sputter-deposited Ru filter anodes composed of a single Ru layer and three Ru layers separated by Nafion-carbon ink, respectively, were compared to Pt, Pt:Ru alloy, and an ink-based Ru filter anodes. The amount of Pt in each anode was 0.15 mg/cm² and the amount of Ru in each Ru-containing anode was 0.080 mg/cm². For an anode feed consisting of hydrogen, 200 ppm CO, and 2% O₂ (in the form of an air bleed), all Ru filter anodes outperformed the Pt:Ru alloy. The performance of the Pt + single-layer sputtered Ru filter was double that of the Pt:Ru alloy (0.205 vs. 0.103 A/cm² at 0.6 V). The performance was also significantly greater than that of the ink-based Ru filter (0.149 A/cm² at 0.6 V). Within the filter region of the anode, it is likely that the decreased hydrogen kinetics of the Ru (compared to Pt) allow for more of the OH_{ads} formed from oxygen in the fuel stream to oxidize adsorbed CO to CO₂.

© 2002 The Electrochemical Society. [DOI: 10.1149/1.1479727] All rights reserved.

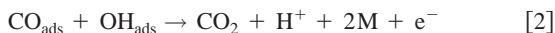
Manuscript submitted August 15, 2001; revised manuscript received January 10, 2002. Available electronically May 15, 2002.

Proton-exchange membrane-based fuel cells (PEMFCs) are gaining popularity due to their high operating efficiency and environmental friendliness. Because of the difficulties inherent to storing hydrogen, hydrocarbon fuels such as propane, natural gas, and gasoline are used to produce reformat gas. Dry reformat is typically composed of 40-75% hydrogen, 15-25% carbon dioxide, 10-10,000 ppm carbon monoxide, and a balance of nitrogen, depending on the fuel processing system used.^{1,2} It has been shown extensively that CO poisons the platinum catalyst used in PEMFC systems.³⁻⁷ Carbon monoxide chemically adsorbs onto available Pt catalyst sites as shown in



As little as 10 ppm CO in the fuel stream can lower the power output of the PEMFC by 50%.^{6,7} For the reforming process to be effective in the fuel cell system, this problem must be solved. Attempts to find catalysts both tolerant to CO and equivalent in performance to Pt have led to the alloying of Pt with Ru, Mo, W, Co, Os, Ir, Ni, and Sn.⁷⁻¹¹ Used by themselves as catalysts, these metals do not provide the high hydrogen activity necessary to achieve the current densities that make PEMFCs competitive in the marketplace.^{9,12,13} The most commonly used alloy is Pt:Ru. The Pt:Ru alloy combines the high catalyst activity of pure Pt with the increased CO tolerance of pure Ru catalyst.¹²⁻¹⁴

The oxidation of CO_{ads} from the Pt:Ru catalyst surface in the anode shown in Eq. 2 follows Langmuir-Hinshelwood kinetics^{12,13}



where M represents Pt or Ru. The reactions by which OH_{ads} is formed on Pt and Ru are shown in Eq. 3^{15,16}

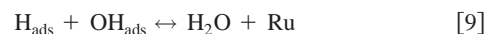


The formation of OH_{ads}, shown in Eq. 3 is the rate-determining step of this reaction and occurs on platinum at potentials of 0.7 V vs.

the reversible hydrogen electrode (RHE) and above.^{13,15,16} Ruthenium has the ability to form OH_{ads} from water at significantly lower potentials than Pt, 0.35 V for 50 atom % Ru and 0.2 V for 90 atom % Ru,^{12,13,16} allowing for a certain amount of CO tolerance. At low temperatures (70-85°C), the Pt:Ru (1:1 atomic ratio) alloy catalyst provides nearly equivalent performance to pure H₂ on Pt for CO concentrations up to 100 ppm in the feedstream.^{8,12}

The injection of oxygen into the fuel stream increases catalyst tolerance to CO.^{14,17} However, even the addition of high levels of oxygen to the feedstream (2-4% by volume of hydrogen) provides approximately 100 ppm CO tolerance. Roughly one out of every 400 O₂ molecules oxidizes an adsorbed CO molecule, with the balance reacting with hydrogen.¹⁴ The placement of a layer of Ru catalyst before the Pt electrode to act as a filter has been shown to increase the effectiveness of oxygen addition over conventional Pt:Ru alloy catalysts.¹⁸ This method also eliminates the process of alloying the Pt and Ru metals, and by using a filter, the Pt loading in the anode is free to be varied.

It is believed that the following mechanism is occurring in the Ru filter for a fully humidified fuel stream containing oxygen, hydrogen, and carbon monoxide^{14,18-33}



Reactions 4, 5, and 6 represent the adsorption of species onto the Ru catalyst. Reaction 7 represents an intermediate reaction on Ru resulting in the formation of OH_{ads}. Reactions 8-11 represent competing desorption reactions on the Ru catalyst. Equation 10 is well documented as following Langmuir-Hinshelwood kinetics on Pt and Ru.^{34,35} Of the desorption reactions, Reactions 8 and 10 are desired

* Electrochemical Society Student Member.

** Electrochemical Society Fellow.

*** Electrochemical Society Active Member.

^z E-mail: white@enr.sc.edu

as they result in the oxidation of CO_{ads} . Earlier work¹⁸ showed that the reaction shown in Eq. 8 is the primary means by which CO_{ads} is oxidized within the filter, resulting in the formation of H^+ . Thus, like the Pt region following the filter, a three-phase interface of catalyst (Ru here), carbon and Nafion are required for the filter to operate. The above mechanism is not a comprehensive list of all reactions occurring within the anode region. The mechanism focuses on those reactions that lead to CO oxidation. For example, evidence has been found that H_2O_2 is formed as an intermediate during oxygen reduction at overpotentials as low as 0.5 V.¹⁹ However, H_2O_2 breaks down to oxygen-containing compounds at or even before reaching the catalyst surface.^{4,7,17}

The goal of this work is to increase the effectiveness of the Ru filter by applying it through sputter deposition as opposed to conventional catalyst ink-based application methods. Sputter deposition is widely used for integrated circuit manufacturing and has been investigated for us in fuel cells for more than a decade.³⁶⁻³⁹ Hirano *et al.*⁴⁰ sputter deposited platinum on uncatalyzed gas-diffusion layers (GDLs) resulting in cell performances at loadings of 0.10 mg Pt/cm² equivalent to those of standard methods at loadings of 0.40 mg Pt/cm². Witham *et al.*⁴¹ achieved direct methanol fuel cell (DMFC) anode catalyst activities one to two orders of magnitude higher than those of conventional ink-based catalysts, suggesting that DMFC anodes may be manufactured containing less than one-tenth the amounts presently used (2.5-4 mg Pt/cm²) without loss in performance. Holleck *et al.*⁴² have sputtered catalyst mixtures at the front surface of the anode electrode. These mixtures included Pt:Ru:X where X represents Ni, Pd, Co, Rh, Ir, Mn, Cr, W, Nb, and Zr. For low levels of CO (10 ppm), specific Pt:W and Pt:Ru:W alloys performed better than Pt:Ru.

In this work, the Ru filter is sputter-deposited as a single layer and as a series of three layers (separated by Nafion-carbon ink) and compared to a conventional ink-based filter. By manufacturing membrane-electrode assemblies (MEAs) composed of multiple sputter-deposited Pt layers, Cha and Lee⁴³ were able to increase the Pt catalyst activity significantly over conventional ink-based MEAs by increasing the amount of Pt in contact with Nafion and carbon. This process was further improved upon by reducing the amount of Nafion-carbon ink (NCI) separating the Pt layers, resulting in thinner, more effective electrodes.⁴⁴ For the same loading of catalyst, sputter-depositing catalyst between layers of NCI increases the active area of the catalyst *vs.* a single sputter-deposited layer.^{43,44} For Pt catalyst, this results in greater performance of the fuel cell electrodes.^{43,44} It is predicted that for the Ru filter, this process will create more sites upon which CO can be oxidized, resulting in a more CO-tolerant PEMFC MEA.

Experimental

Development of ink-based MEAs.—The method described in U.S. Patent 5,211,984 provides an outline for the catalyst ink preparation and MEA fabrication performed in this project.⁴⁵ The following catalyst inks were prepared: (i) Nafion + carbon only (Nafion-carbon Ink or NCI), (ii) Nafion + 20% Pt on carbon, (iii) Nafion + 20% Pt:Ru on carbon, and (iv) Nafion + 20% Ru on carbon.

The inks were prepared for Pt, Pt:Ru, Ru by adding the E-TEK catalyst (20% catalyst on XC-72 Carbon) to a solution of 5 wt % Nafion (DuPont). For NCI, XC-72 Carbon was added to a solution of 5 wt % Nafion.

Decals (Teflon, 10 cm², three-ply) were weighed prior to application of catalyst ink. The ink was drawn across the surface of the decals using a Meyer rod. The coated decals were dried in an oven at 105°C under ambient pressure for 10 min.

Target loadings were 0.15 mg Pt/cm² (anode), 0.230 mg Pt:Ru/cm² (anode), and 0.15 mg Pt/cm² (cathode). Target loadings of 0.230 mg Pt:Ru/cm² and of 0.080 mg Ru/cm² for the Ru filter were chosen so that a 1:1 atomic ratio of Pt:Ru is maintained, while Pt catalyst is maintained at a loading of 0.15 mg/cm².

Table I. Types of ink-based MEUs tested.

MEU name	Description
Pt	0.15 mg Pt/cm ² anode 0.15 mg Pt/cm ² cathode Uncatalyzed Toray GDLs on anode and cathode
Pt:Ru	0.23 mg Pt:Ru/cm ² anode 0.15 mg Pt/cm ² cathode Uncatalyzed Toray GDLs on anode and cathode
Pt + Ru (Ru filter)	0.15 mg Pt/cm ² anode 0.15 mg Pt/cm ² cathode 0.080 mg Ru/cm ² coated Toray GDL on the anode Uncatalyzed Toray GDL on the cathode side

To form a MEA with ink-coated decals, appropriate decals were placed on either side of the PEM (Nafion 117, protonated form). This assembly was hot-pressed to ensure bonding. It was then cooled to room temperature, before the decals were carefully peeled from the assembly.

To form a membrane-electrode unit (MEU, equivalent to a GDL + MEA + GDL) with ink-coated GDLs, appropriate GDLs were placed on either side of a PEM (Nafion 117, protonated form, soaked in deionized water for 1 h). This assembly was hot-pressed to ensure a well-bonded MEU. The types of ink-based MEUs made are shown in Table I.

Development of sputter-deposition-based MEAs.—Plasma modifications and sputter-deposition augmentations/additions were both completed using an Anatech Hummer 10.2 sputter-coating tool. A modified sample stage was used to support Nafion 117 substrates up to 6 × 6 cm while masking 1.5 cm about the membrane's perimeter.

It has been shown previously that alternating current (ac) plasma should be used for all plasma modifications, as Nafion 117 and MEAs from Nafion 117 suffer no ill effects from this treatment.⁴⁴ An aluminum target was used for ac plasma modifications, while the Ru (Kurt J. Lesker) target and carbon evaporation system (Anatech) were used for sputter augmentations/additions.

All MEAs subject to sputter deposition were first ac plasma cleaned for 5 min at 5 mA and 1.2 kV to remove residual buildup from the target as well as roughen the substrate surface. All treatments were completed at ~62 mTorr. A separate vacuum chamber was used to evacuate each substrate to ~45 mTorr, before it was placed in the sputter-coating tool to minimize contaminant outgassing in the deposition chamber. A potential of 1.8 kV and a current of 8 mA were maintained to control the deposition rate for Ru. A SiO₂ sample was sputter-deposited *in situ* with each MEA. The resultant metal/SiO₂ stack was subjected to cross-sectional view scanning electron microscopy (SEM) imaging to verify the thickness of the sputter-deposited film and top-view SEM imaging to determine surface characteristics of the film.

Multilayered Ru filters were manufactured by a method similar to that described by Cha and Lee.⁴³ On the MEA anode, a layer of NCI was sprayed on the surface of the sputter-deposited Ru layer. The MEA was then dried at 80°C under vacuum for 10 min. Additional layers of sputter-deposited Ru and NCI were added until the desired Ru loading and number of Ru layers were attained.

MEAs containing sputter-deposited catalyst layers were manufactured into MEUs through similar methods as the ink-based MEAs.

Cell assembly and testing.—The MEUs were placed in a 10 cm² cell assembly and incubated for 4 to 8 h at ambient pressure, cell temperature of 70°C, stoichiometric ratio ([actual flow]/[stoichiometric flow] required for a 1.0 A/cm² current) of 1.5 at the anode and 2.0 at the cathode. Fuel cell performance curves were obtained under the conditions given in Table II.

Table II. Fuel cell test conditions.

Pressure	1 atm
Cell temperature	70°C
Stoichiometric ratio (at 1 A/cm ²)	1.5 hydrogen 2.0 air
Feedstreams	Anode: hydrogen, H ₂ + CO, H ₂ + CO + air bleed Cathode: air
Humidification	Complete humidification of anode and cathode gas streams for all trials
Air bleed	2.0% O ₂ (in the form of an air bleed relative to the volumetric flow of hydrogen in slm)
CO amounts	50, 200 ppm

Results

Determination of sputter-deposition rates and catalyst loading.—The sputter-deposition rates for Ru were determined with loadings calculated from cross-sectional and top-view SEM images of sputter-deposited Ru films on SiO₂ substrates. The top-view SEM images in Fig. 1 were analyzed to determine the surface coverage of the sputter-deposited film (Pt ~ 65%, Ru ~ 56%). Ru did not form a continuous film on the SiO₂ substrate, but rather agglomerated. This is consistent with literature.⁴⁶ The surface coverages were used in conjunction with the bulk density of Ru (12.2 g/mL) and the film thicknesses from the cross-sectional SEM images to calculate the subsequent Ru loadings. The Ru sputter-deposition rate was constant with time at 3.3 μg Ru/cm²/min.

The cross-sectional view in Fig. 1 shows that the thickness of 30 and 45 min sputter-deposited Ru is roughly two and three times the thickness of a 15 min deposition of Ru, respectively. Semiquantitative analyses via energy dispersive X-ray spectroscopy (EDXS) and Rutherford backscattering spectrometry (RBS) confirm these Pt and Ru deposition rates.

CO testing.—The three types of Pt + Ru filter anodes prepared are shown in Fig. 2. They were made to the following specifications: filter 1: 0.08 mg/cm² ink-based 20% Ru/C, filter 2: NCI + 25 min (0.08 mg/cm²) of sputter-deposited Ru, and filter 3: NCI + 3 × (8.33 min of sputter-deposited Ru + NCI). The total Ru loading was 0.08 mg/cm².

Filter 1 is an ink-based Ru filter, while filter 2 and 3 are comprised of one and three layers of a sputter-deposited Ru, respec-

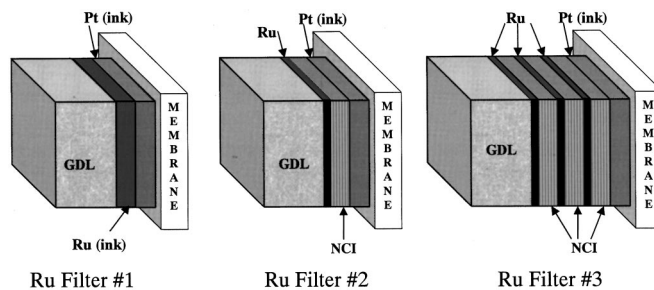


Figure 2. Diagram of the Ru filtered anode. The filter is a layer of Ru catalyst placed between the Pt catalyst and the gas-diffusion layer for oxidizing CO present within the anode. Filter 1 is the standard Ru filter prepared from a catalyst ink. Filter 2 is a single sputter-deposited layer of Ru separated from the Pt electrode by a layer of NCI. Filter 3 is a three-layer sputter-deposited Ru filter separated from the Pt electrode by a layer of NCI. All filters have a loading of 0.08 mg Ru/cm² and were placed atop a Pt electrode with a loading of 0.15 mg Pt/cm².

tively. As shown in Fig. 2, NCI is used to separate the layers of sputter-deposited Ru layered between Nafion-carbon ink (NCI).

Figure 3 compares various Ru filters to the Pt:Ru alloy and the baseline MEA at 70°C for an anode feed of hydrogen + 50 ppm CO. All MEAs prepared with Pt, Pt:Ru alloy, and Pt + Ru filters 1-3 exhibited a dramatic loss of performance when 50 ppm CO was added to the hydrogen feedstream. In all cases, fuel cell performance dropped to less than 40% of the baseline MEA running on pure hydrogen fuel. It is clear that the filters do not completely oxidize the CO in the feedstream to CO₂. The remaining CO passes through the filter and poisons the Pt portion of the anode, resulting in performance resembling that of a typical Pt anode as evidenced in Fig. 3. The Pt:Ru alloy demonstrates CO tolerance over a Pt anode consistent with literature, more than doubling the current density of any other anode configuration at 0.6 V.

When 2% O₂ (in the form of an air bleed) is added to the anode feed, all Ru-containing anodes show significant performance improvement over the Pt baseline as shown in Fig. 4. For the 25 min Ru (0.08 mg Ru/cm²) sputter-deposited filter, there is almost no performance loss except at lower voltages. The Pt:Ru alloy and standard Ru filter show almost identical performance, roughly 20% less than the baseline (0.227 vs. 0.275 A/cm² at 0.6 V). The performance of the Ru filter cannot be explained by the formation of a Pt:Ru alloy as there is no interface between Pt and Ru. A layer of NCI separates the sputter-deposited Ru from the Pt electrode for the sputter-deposited Ru filters. The multilayered filter performed the

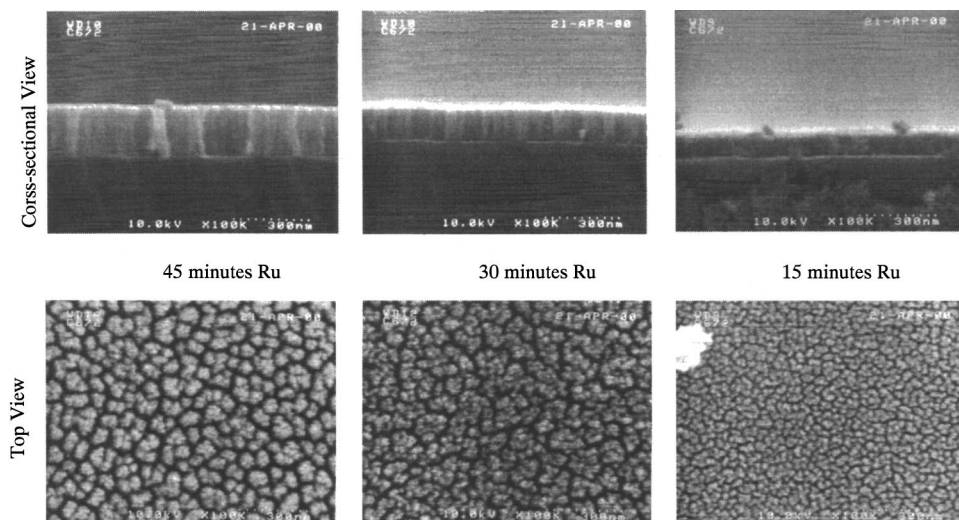


Figure 1. Top and cross-sectional SEM images of sputter-deposited Ru on Si/SiO₂ substrates.

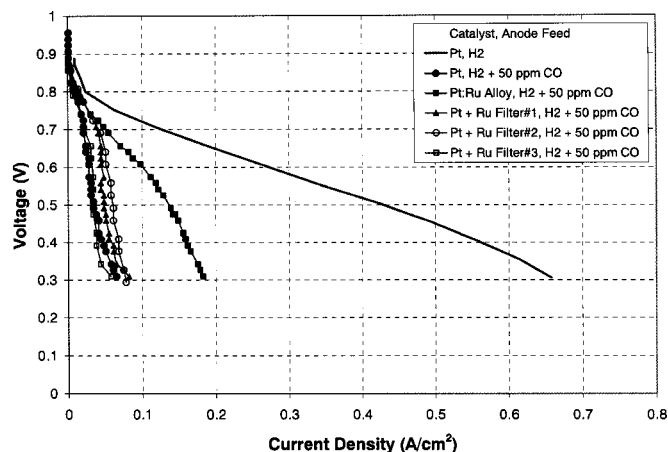


Figure 3. Performance comparison of MEUs with sputter-deposited Ru filter under $H_2 + 50$ ppm CO conditions. $P = 1$ atm, $T = 70^\circ\text{C}$. The filter configurations are defined as follows: filter 1 (\blacktriangle) is the standard Ru filter prepared from an ink; filter 2 (\circ) is a single 25 min sputter-deposited layer of Ru separated from the Pt electrode by a layer of NCI; filter 3 (\square) is a three-layer sputter-deposited Ru filter (8.33 min per layer, see Fig. 2 for design) separated from the Pt electrode by a layer of NCI.

worst of the Ru-containing anodes. This is likely due to the increased diffusional resistances caused by the thickness of the Ru filter.

As the amount of CO is increased from 50 to 200 ppm, the benefit of the Ru filters is seen more clearly. Figure 5 shows that all three Ru filter types outperform the Pt:Ru alloy. For the anode consisting of Pt + Ru filter 2, the performance is double that of the Pt:Ru alloy (0.205 vs. 0.103 A/cm^2 at 0.6 V). The MEA containing filter 2 loses only 20% of its performance (0.255 vs. 0.205 A/cm^2 at 0.6 V) as the CO concentration is increased from 50 to 200 ppm CO, and loses only 25% vs. the hydrogen baseline. There have been other reports of 200 ppm CO tolerance with an air bleed, but the conditions involved higher temperatures and higher loadings.¹⁴ The MEA containing filter 2 significantly outperformed ink-based filter 1 by more than 35% (0.205 vs. 0.149 A/cm^2 at 0.6 V). These results also constitute a significant improvement over the previous work done on the Ru filter.¹⁸ Under conditions identical to those shown in Table II, the Ru filter of 0.21 mg/cm^2 developed in Ref. 18 showed an equivalent loss in performance to filter 2 of this work when only 100 ppm CO was added to the anode feed containing 2% O_2 in the form

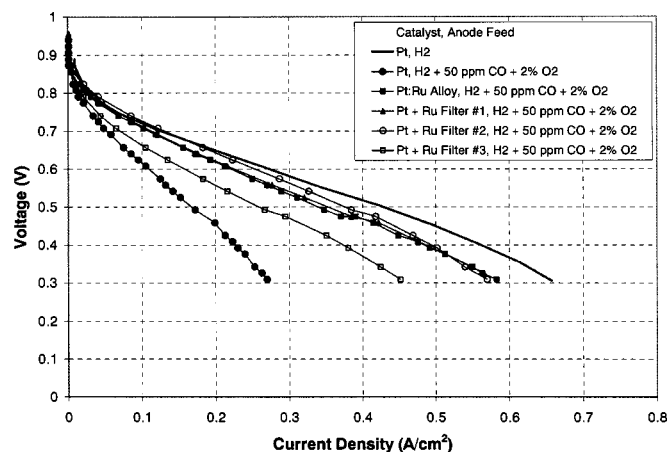


Figure 4. Performance comparison of MEUs with sputter-deposited Ru filter for an anode feed of hydrogen + 50 ppm CO + 2% O_2 . $P = 1$ atm, $T = 70^\circ\text{C}$. The filter configurations are defined in Fig. 3.

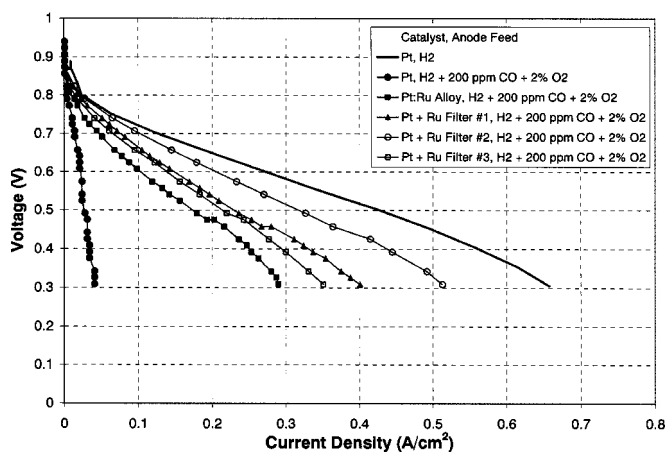


Figure 5. Performance comparison of MEUs with sputter-deposited Ru filter for an anode feed of hydrogen + 200 ppm CO + 2% O_2 . $P = 1$ atm, $T = 70^\circ\text{C}$. The filter configurations are defined in Fig. 3.

of an air bleed. The Ru filter in Ref. 18 showed a 50% loss in performance when the CO concentration was doubled to 200 ppm.

Of the three Ru-filtered MEAs tested, filter 3 performed the worst at 200 ppm CO, but suffered only a 12% loss compared to its performance at 50 ppm CO (0.138 vs. 0.157 A/cm^2 at 0.6 V). That there is so little drop-off from this three-layer filter configuration suggests that the lower performance compared to the single-layer sputter-deposited filter 2 is due to diffusional resistances caused by the increased thickness of this filter. The layers of NCI are very thick relative to each Ru deposition (~ 40 nm for each sputter-deposited Ru layer compared to ~ 12 μm for each NCI layer),⁴⁴ accounting for more than 99.5% of the Ru filter layer thickness. The increased thickness of this three-layer filter requires hydrogen to travel further to reach the Pt vs. a single-layer filter, and vs. the baseline MEA giving rise to greater diffusional resistances. By reducing the amount of NCI used in each sputter-deposited layer (by diluting the NCI), a thinner, more effective multilayered Ru filter may be developed.

The addition of a layer of NCI between the Pt electrode and the sputter-deposited Ru filter is evidence that the CO oxidation is not the result of a layer of Pt:Ru alloy being formed at the interface of the filter and the Pt electrode. Thus, it can be hypothesized that the CO oxidation is occurring very fast in relation to the diffusion of the gases through the filter region. Nearly all the CO is oxidized within a region ~ 100 to 120 nm thick (see Fig. 1). Therefore, it is assumed that a filter of identical loading (0.08 mg/cm^2) would perform similarly in front of a Pt electrode of any loading.

It is assumed that all oxygen reacts almost immediately within the filter region and that the hydroxyl groups produced then react with CO to produce CO_2 . Even with 200 ppm CO tolerance, only one out 200 O_2 molecules is being used to oxidize CO. Further research into catalysts with lower activity than Ru with respect to hydrogen may provide even further CO oxidation by further shifting the selectivity of the oxygen reactions toward the oxidation of CO to CO_2 .

Conclusions

The sputter-deposited Ru filters developed here, containing less than 40% the amount of Ru (0.080 vs. 0.21 mg/cm^2) of the previous work,¹⁸ achieved twice the CO tolerance (200 ppm CO vs. 100 ppm CO) under similar operating conditions ($H_2 + 2\%$ O_2 anode feed, a cathode feed of air, 70°C operating temperature).

For an anode feedstream consisting of hydrogen, 200 ppm CO, and 2% oxygen, all MEAs containing Pt + Ru filter anodes showed increased CO tolerance compared to a Pt:Ru alloy containing similar amounts of Pt and Ru (0.150 and 0.080 mg/cm^2 , respectively). The

MEA containing a single sputter-deposited Ru filter exhibited greater CO tolerance than that of the MEA containing the ink-based Ru filter (0.205 vs. 0.149 A/cm² at 0.6 V).

Attaining 200 ppm CO tolerance by using 2% oxygen is equivalent to one out 200 O₂ molecules being used to oxidize CO_{ads} molecule, while the rest likely react with H⁺ to form water. Catalysts with characteristics similar to Ru but with lower hydrogen activity would likely allow for a higher percentage of oxygen in the feed-stream to react with adsorbed CO, resulting in a more effective filter.

While the three-layered sputter-deposited Ru filter (filter 3) performed the worst of the three filters, its drop in performance (12%) as the CO in the anode feed was increased from 50 to 200 ppm (balance H₂ + an air bleed containing 2% O₂) was the smallest of all the anodes tested. NCI accounts for 99.7% of the multilayered Ru filter thickness. Further research can be done to optimize this three-phase interface area of the Ru filter and eliminate the unused portion of the electrode, resulting in thinner, more effective filters. However, to generate a filter with a high number of Ru layers is neither the most economical (due to the time required to generate such a multilayered MEA) nor most effective approach. The generation of a continuous three-phase interface is the ultimate goal of this method and this is what should be pursued using the method of sputter deposition. Simultaneously sputter-depositing Ru and spray depositing NCI could produce a continuous three-phase interface region. This would result in an extremely thin (~1 μm) filter that may provide high Ru activity with minimal diffusional resistances. And by applying this Ru/C/Nafion filter in a single application to the PEM, the process is less time-consuming and thus more economical.

Because benefits of the Ru filter occur at high level air bleed (2% O₂) and the Pt:Ru alloy provides CO tolerance even without air bleed, it is suggested that the anode configuration that would provide optimal CO tolerance would consist of a sputter-deposited Ru filter placed in front of and adjacent to a Pt:Ru alloy.

Acknowledgments

The authors acknowledge financial support from the National Institute of Standards and Technology under cooperative agreement no. 70NANB8H4039.

The University of South Carolina assisted in meeting the publication costs of this article.

References

- M. A. Inbody, N. E. Vanderborgh, J. C. Hedstrom, and J. I. Tafaye, *Fuel Cell Seminar*, P, 624 (1996).
- Y.-L. Cheng, L.-D. Chen, and J. P. Seaba, *Fuel Cell Power for Transportation*, SAE SP-1425, 55 (1999).
- H. P. Dhar, L. G. Christner, A. K. Kush, and H. C. Maru, *J. Electrochem. Soc.*, **133**, 1574 (1986).
- H. F. Oetjen, V. M. Schmidt, U. Stimming, and F. Trila, *J. Electrochem. Soc.*, **143**, 3838 (1996).
- H. P. Dhar, L. G. Christner, and A. K. Kush, *J. Electrochem. Soc.*, **134**, 3021 (1987).
- B. N. Grgur, N. M. Markovic, and P. N. Ross, *J. Electrochem. Soc.*, **146**, 1613 (1999).
- R. J. Bellows, E. P. Marucchi-Soos, and D. T. Buckley, *Ind. Chem. Eng. Rev.*, **35**, 1235 (1996).
- M. Iwase and S. Kawatsu, in *Proton-Conducting Membrane Fuel Cells I*, S. Gottesfeld, G. Halpert, and A. Landgrebe, Editors, PV 95-23, p. 12, The Electrochemical Society Proceedings Series, Pennington, NJ (1995).
- M. Watanabe, H. Igarashi, and T. Fujino, *J. Electroanal. Chem.*, **67**, 1194 (1999).
- B. N. Grgur, N. M. Markovic, and P. N. Ross, Jr., in *Proton-Conducting Membrane Fuel Cells II*, S. Gottesfeld and T. F. Fuller, Editors, PV 98-27 p. 176, The Electrochemical Society Proceedings Series, Pennington, NJ (1999).
- A. B. Anderson, E. Grantscharova, and P. Schiller, *J. Electrochem. Soc.*, **142**, 1880 (1995).
- H. A. Gasteiger, N. M. Markovic, and P. N. Ross, Jr., *J. Phys. Chem.*, **99**, 8290 (1995).
- H. A. Gasteiger, N. M. Markovic, P. N. Ross, Jr., *J. Phys. Chem.*, **99**, 16757 (1995).
- R. J. Bellows, E. Marucchi-Soos, and R. P. Reynolds, *Electrochem. Solid-State Lett.*, **1**, 69 (1998).
- K. Wang, H. A. Gasteiger, N. M. Markovic, and P. N. Ross, Jr., *Electrochim. Acta*, **41**, 2587 (1996).
- M. T. M. Koper, J. J. Lukkien, A. P. J. Jansen, and R. A. van Santen, *J. Phys. Chem.*, **103**, 5522 (1999).
- V. M. Schmidt, H.-F. Oetjen, and J. Divisek, *J. Electrochem. Soc.*, **144**, L237 (1997).
- A. Haug, R. E. White, J. W. Weidner, W. Huang, *J. Electrochem. Soc.*, **149**, A862 (2002).
- N. M. Markovic, T. J. Schmidt, V. Stamenkovic, and P. N. Ross, *Fuel Cells*, **1**, 105 (2001).
- N. M. Markovic, B. N. Grgur, C. A. Lucas, and P. N. Ross, *J. Phys. Chem. B*, **103**, 487 (1999).
- K. Bleakley and P. Hu, *J. Am. Chem. Soc.*, **121**, 7644 (1999).
- C. Zhang, P. Hu, and A. Alavi, *J. Am. Chem. Soc.*, **121**, 7931 (1999).
- S. H. Oh and R. M. Sinkevitch, *J. Catal.*, **142**, 254 (1993).
- N. M. Markovic, T. J. Schmidt, B. N. Grgur, H. A. Gasteiger, R. J. Behm, and P. N. Ross, *J. Phys. Chem.*, **103**, 8568 (1999).
- E. Yeager, *J. Mol. Catal.*, **38**, 5 (1986).
- E. Yeager, *Electrochim. Acta*, **29**, 1527 (1984).
- A. Alavi, P. J. Hu, T. Deutsch, P. L. Silvestrelli, and J. Hutter, *Phys. Rev. Lett.*, **80**, 3650 (1998).
- H.-I. Lee, G. Praline, and J. M. White, *Surf. Sci.*, **91**, 581 (1980).
- H. A. Gasteiger, N. Markovic, P. N. Ross, and E. J. Cairns, *J. Phys. Chem.*, **98**, 617 (1994).
- S. Wasmus and A. Küver, *J. Electroanal. Chem.*, **461**, 14 (1999).
- P. Ferreira-Aparicio, A. Guerrero-Ruiz, and I. Rodriguez-Ramos, *Appl. Catal., A*, **170**, 177 (1998).
- P. Ferreira-Aparicio, I. Rodriguez-Ramos, J. A. Anderson, and A. Guerrero-Ruiz, *Appl. Catal., A*, **202**, 183 (2000).
- P. Freni, G. Calogero, and S. Cavallaro, *J. Power Sources*, **87**, 28 (2000).
- P. J. Berlowitz, C. H. F. Peden, and D. W. Goodman, *J. Phys. Chem.*, **92**, 5213 (1998).
- R. Imbuhl, M. P. Cox, and G. Ertl, *J. Chem. Phys.*, **83**, 1578 (1985).
- E. A. Ticianelli, C. R. Derouin, and S. Srinivasan, *J. Electroanal. Chem.*, **251**, 275 (1988).
- S. Srinivasan, D. J. Manko, J. Koch, M. A. Enayetullah, and A. J. Appleby, *J. Power Sources*, **29**, 367 (1990).
- E. A. Ticianelli, C. R. Derouin, A. Redondo, and S. Srinivasan, *J. Electrochem. Soc.*, **135**, 2209 (1988).
- S. Mukerjee, S. Srinivasan, and A. J. Appleby, *Electrochim. Acta*, **38**, 1661 (1993).
- S. Hirano, J. Kim, and S. Srinivasan, *Electrochim. Acta*, **42**, 1587 (1997).
- C. K. Witham, W. Chun, T. I. Valdez, and S. R. Narayanan, *Electrochem. Solid-State Lett.*, **3**, 497 (2000).
- G. L. Holleck, D. M. Pasquariello, and S. L. Clauson, in *Proton-Conducting Fuel Cells II*, S. Gottesfeld and T. F. Fuller, Editors, PV 98-27, p. 150, The Electrochemical Society Proceedings Series, Pennington, NJ (1999).
- S. Y. Cha and W. M. Lee, *J. Electrochem. Soc.*, **146**, 4055 (1999).
- A. T. Haug, R. E. White, J. W. Weidner, W. Huang, S. Shi, T. Stoner, and N. Rana, *J. Electrochem. Soc.*, **149**, A280 (2002).
- M. S. Wilson, U.S. Pat. 5,211,984 (1993).
- J. A. Poirier and G. E. Stoner, *J. Electrochem. Soc.*, **141**, 425 (1994).